Fractional impedance of supercapacitor: an extended investigation

Ravneel Prasad, Utkal Mehta & Kajal Kothari

ONLINE FIRST

International Journal of Dynamics and Control

ISSN 2195-268X

Int. J. Dynam. Control
DOI 10.1007/s40435-020-00735-7

Springer

International Journal of Dynamics and Control
https://doi.org/10.1007/s40435-020-00735-7

Fractional impedance of supercapacitor: an extended investigation

Ravneel Prasad[1] · Utkal Mehta[1] · Kajal Kothari[1]

Received: 13 August 2020 / Revised: 31 October 2020 / Accepted: 16 November 2020

Abstract

There has been an impressive growth rate of supercapacitor's applications, which urges a need for an in-depth investigation on modeling of supercapacitor in order to study the behavior and designing systems integrated with it. Studies have been carried out in multiple domains, but the time domain based modeling has been a simple and commonly adopted study. This research proposes the block-pulse based identification method for modeling the time response behavior of the supercapacitor. The proposed method for modeling supercapacitor simplifies fractional derivative into simple algebra rather than direct complex function like the Mittag-Leffler function. Furthermore, in this paper the critical observation is conducted with varied time duration of data collected for modeling of the supercapacitor of same brand and capacity. It shows how its parameters are affected by time length despite capturing full charge and discharge cycles. This may help in the crucial stage of determining the sample size or the data length for which modeling is to be performed. Some recommendations have been made after systematic observations on three different branded supercapacitors of same capacitance. Using the proposed technique, one can estimate the model parameters set to handle complexity posed by fractal behavior of supercapacitors.

Keywords Supercapacitor · Impedance model · Fractional calculus · Time domain analysis · Block-pulse function · Operational matrix

1 Introduction

Supercapacitor is an energy storage component that bridges the gap between standard batteries and conventional capacitors. It is able to store or dissipate large amounts of energy in a short span of time. The supercapacitor, also known as double-layer capacitor or ultracapacitor, can be categorized into two different classes depending on how the charges are stored in the system. A class of Electrostatic Double Layer Capacitor (ELDC) stores energy in a non-faradic process and does not involve any chemical reaction. On the other hand, Pseudo Capacitor is based on a faradic redox reaction which involves transfer of charges between the electrode and electrolyte [1]. Hence, depending on the capacitance and time response, it can be used in electric cars, renewable energy systems, biomedical sensors, memory backup, power regulators and etc. It is true that supercapacitor's properties such as longer lifespan, greater power density over batteries and high energy density over conventional capacitors, are useful enough to replace the batteries in hybrid vehicles and power backup systems [1–4].

The aforementioned properties has been studied rigorously by researchers to understand internal behavior through modeling. In recent times, fractional calculus has emerged as a popular concept in modeling. Phenomena such as anomalous relaxation and diffusion process which are difficult to be described through modeling using conventional calculus, in such situations fractional calculus comes to aid. The validity of fractional calculus could be seen in study of fluid dynamics [5], quantum mechanics [6], power and energy of energy storage components [7], biological impedance modeling[8], dielectric relaxation of materials [9], electromagnetic wave propagation [10], frequency regulation in AC microgrids [11], adaptive control for unknown systems with measurement errors [12] and many others. Fractional calculus based modeling has been known to represent complex systems with reduced number of parameters and improves the robustness

✉ Utkal Mehta
utkal.mehta@usp.ac.fj

Ravneel Prasad
ravneel.r.prasad@usp.ac.fj

Kajal Kothari
kajal.kothari@usp.ac.fj

1 School of Engineering and Physics, The University of the South Pacific, Laucala Campus, Suva, Fiji

Published online: 27 November 2020

in control designing due to the non-locality and long memory nature [13,14].

Supercapacitor has also been explored with fractional calculus to cover the phenomenon of dispersion caused by porosity, inhomogenity, fractal/rough geometry and distributed surface reactivity [15]. Thus, in impedance modeling, a constant phase element (CPE) is used to describe these phenomena which has the impedance as given below.

$$Z_{CPE} = \frac{1}{Cs^{\alpha}} \tag{1}$$

where C is fractional capacitance, also called the pseudo-capacitance with units $F/s^{1-\alpha}$ (the s in the unit represents time) and $0 \leq \alpha \leq 1$ is the order.

A simple R-C (resistor-capacitor) based fractional model has been analyzed in [16,17] based on Riemann-Liouville and Grunwald-Letnikov definitions, respectively. The same model was used in [18–20], where MLF based model was analyzed in time domain. Similar analyses using the MLF function based on a parallel R-C model with a series resistance have been done in [21]. An extended parallel R-C model was used in [4] to study the variance in model for different types of capacitors. In [22] parallel R-C ladder model was investigated for performance in time domain. Moreover, Bertrand et. al in [23], synthesized a nonlinear model performing frequency analysis. A simple model with single resistor in series with three different fractional ordered capacitance which provided much more dynamic compared to a simple RC model was analyzed for frequency response in [24,25]. Frequency domain based modeling was also studied in [26,27]. Through all these literature, it has been effectively outlined the evolution of fractional modeling for supercapacitors.

The physical and geometric interpretation of fractional model not being distinct when compared to integer models makes fractional model's system identification critical. Various fractional supercapacitor impedance models have been studied in both time and frequency domain, however, the use of operational matrix based modeling of supercapacitor has not been studied. The use of operational matrix in handling the fractional order derivative or integration (FOD/FOI) reduces the computational complexity by converting the complex fractional derivative equations into simple algebraic form [28–31]. The use of block-pulse function is proposed in this research to estimate the FOD/FOI based time domain response for the supercapacitor. Furthermore, new investigation is performed on the variability of supercapacitor's parameters based on time dependency. The comparison of estimated fractional supercapacitor model with respect to different time stamp data sets has been evaluated to study the effect of parameter estimation for a particular supercapacitor. Three different supercapacitors of different brands and values have been experimented upon for this purpose. A useful remark is provided to deal with unpredictable phenomenon of supercapacitor. It suggests there is a stable parameter region for estimation of the fractional impedance values which could help in determining the appropriate data length for modeling. This is in addition with the demonstration of accurate estimation of impedance model for supercapacitor using a simple time domain output expression.

2 Block pulse operational matrix of fractional derivative

The block pulse function (BPF) has shown the quality in systems' analysis, synthesis, and identification [31,32]. The key concept was to transform fractional derivative operation into a simple algebraic form so that the long complex calculations posed due to fractional calculus' long memory property is minimised. The BPF comprises of orthogonal piecewise functions of constant values which is defined over the time interval $[0, T]$ as

$$\phi_i(t) = \begin{cases} 1, & \frac{i-1}{M}T \leq t \leq \frac{i}{M}T \\ 0, & elsewhere \end{cases} \tag{2}$$

where $i = 1, 2, 3, \ldots, M$ with M being the number of elementary functions used. Consider any function, $x(t)$, differential over the time interval $[0, T]$ then it could be represented in terms of BPF as follows:

$$x(t) \cong X^T \phi_{(M)}(t) = \sum_{i-1}^{M} X_i \phi_i(t) \tag{3}$$

where T denotes transpose, $X^T(t) = [X_1, X_2, \ldots, X_M]$ is coefficient vector and $\phi^T{}_{(M)}(t) = [\phi_1(t), \phi_2(t), \ldots, \phi_M(t)]$ is the BPF vector. Accordingly, the fractional derivative can be written in matrix form as below.

$$(\partial^{\alpha} \phi_{(M)})(t) \approx B^{\alpha} \phi_{(M)}(t) \tag{4}$$

In the expression (4), B^{α} is generalized operational matrix of fractional derivative of order α defined as $B^{\alpha} = (F^{\alpha})^{-1}$. The function F^{α} is expressed as,

$$F^{\alpha}_{M\times M} = \left(\frac{T}{M}\right)^{\alpha} \frac{1}{\Gamma(\alpha+2)} \begin{pmatrix} f_1 & f_2 & f_3 & \ldots & f_M \\ 0 & f_1 & f_2 & \ldots & f_{M-1} \\ \vdots & \ddots & f_1 & \ldots & f_{M-2} \\ \vdots & & \ddots & \ddots & \vdots \\ 0 & \ldots\ldots & 0 & & f_1 \end{pmatrix}_{(M\times M)} \tag{5}$$

where $f_1 = 1$, $f_q = q^{\alpha+1} - 2(q-1)^{\alpha+1} + (q-2)^{\alpha+1}$ and $q = 2, 3, \ldots, M$.

Using equations (3) and (4), fractional derivative of any differential functional can be written as:

$$(\partial^\alpha x)(t) \approx X^T B^\alpha \phi_{(M)}(t) \tag{6}$$

This form of differentiation in (6) simplifies the complex calculations of fractional derivative in to simple algebraic operation of matrix multiplication. According to [31], using this form of representation also helps identification of the fractional system of arbitrary order as no restrictions are levied on to the value of α.

In Sect. 4, the modeled supercapacitor output voltage in terms of fractional derivative operation will be converted into algebraic operation using the block pulse generalized matrix of differentiation.

3 Impedance structure

A supercapacitor of either of the two classes mentioned above contains a series resistance (R_s) and capacitor (C). The series model compensates for the total resistance and capacitance of the supercapacitor. However, there is another resistance (R_p) which in parallel to the series model to compensate for the leakage/losses. It is very common phenomenon in capacitor. Leakages usually happen due to faradic and parasitic redox reactions involving impurities, non-uniformity of charge acceptance along the surface of electrode pores and possibility of short-circuit between the anode and cathode due to improper sealing of bipolar electrodes [33,34]. The complete model for supercapacitor is shown in Fig. 1.

The total impedance of the supercapacitor model represented in Fig. 1 can be written mathematically in Laplacian as below.

$$Z(s^\alpha) = \frac{Cs^\alpha (R_s) + 1}{\frac{1}{R_p} + Cs^\alpha \left(\frac{R_s}{R_p} + 1\right)} \tag{7}$$

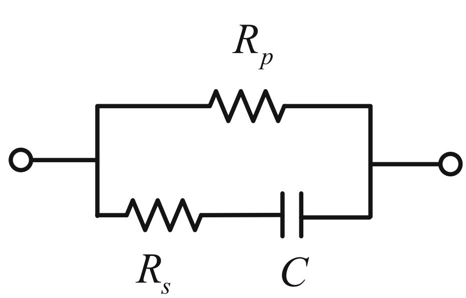

Fig. 1 Supercapacitor model

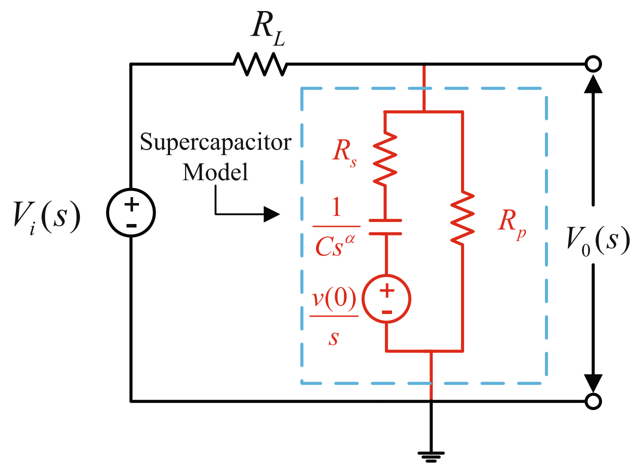

Fig. 2 Supercapacitor charging circuit

Equation (7) can be estimated using the proposed technique mentioned in Sect. 3, an indirect impedance measurement. At times due to some reason, expensive and sophisticated devices such as electro-chemical impedance spectroscopy device are not available. Therefore, an indirect method of obtaining impedance is quite useful and hands on solution. In particular, measurement circuit with voltage or current responses is simple and convenient with basic instruments available. In following, the proposed technique is discussed to measure the fractional impedance and its parameters.

4 Proposed method

The supercapacitor can be connected to a power source V_i, through a load resistance R_L. The resistance R_L can also act as a load to discharge the supercapacitor. For the charging circuit shown in Fig. 2, if the current charging the supercapacitor is $I(s)$ then the output voltage V_o, is given as (8).

$$V_o(s) = V_i(s) - I(s)R_L \tag{8}$$

Now using the Caputo's derivative of an arbitrary function $f(t)$ and its Laplace transform defined in (9) and (10) respectively [4], the current $I(s)$ could be determined.

$$(\partial_c^\alpha f)(t) = \frac{1}{\Gamma(n-\alpha)} \int_0^t \frac{f^{(n)}(\tau)}{(t-\tau)^{\alpha-n+1}} d\tau \tag{9}$$

$$L\left[(\partial_c^\alpha f)(t)\right] = s^\alpha F(s) - \sum_{k=0}^{n-1} s^{\alpha-k-1} f^k(0) \tag{10}$$

where the subscript c indicates Caputo derivative, $\Gamma(.)$ is the Euler's gamma function defined in (11) and $n-1 \le \alpha \le n$

$(n \in N)$.

$$\Gamma(x) = \int_0^\infty e^{-t}\, t^{x-1}\, dt, \quad x \in R^+ \tag{11}$$

Performing circuit analysis on the circuit shown in Fig. 2, the current $I(s)$ can be determined as

$$I(s) = \frac{\frac{V_i(s)}{R_p} + Cs^\alpha\left(\frac{V_i(s)R_s}{R_p} + V_i(s)\right) - Cs^{\alpha-1}V(0)}{\left(1 + \frac{R_L}{R_p}\right) + Cs^\alpha\left(R_s + \frac{R_L R_s}{R_p} + R_L\right)} \tag{12}$$

Substituting equation (12) in equation(8), the the equation for output voltage could be rewritten as (13).

$$V_o(s) = \frac{V_i(s) + Cs^\alpha\,(V_i(s)R_s) + s^{\alpha-1}(CR_L v(0))}{\left(1 + \frac{R_L}{R_p}\right) + Cs^\alpha\left(R_s + \frac{R_L R_s}{R_p} + R_L\right)} \tag{13}$$

After expanding and then further simplifying expression (13), we get

$$\begin{aligned} &V_o(s)\left[(R_p + R_L) + Cs^\alpha\left(R_s R_p + R_L R_s + R_L R_p\right)\right] \\ &= V_i(s)R_p + V_i(s)Cs^\alpha R_s R_p + R_p s^{\alpha-1} CR_L v(0) \end{aligned} \tag{14}$$

Dividing the whole equation by $(s^{\alpha-1})$ and further simplification gives

$$\begin{aligned} &V_o(s)\left[s^{1-\alpha}\left(R_p + R_L\right) + Cs\left(R_s R_p + R_L R_s + R_L R_p\right)\right] \\ &= s^{1-\alpha} V_i(s) R_p + V_i(s) Cs R_s R_p + R_p C R_L v(0) \end{aligned} \tag{15}$$

The expression (15) can be written in time domain differential form as below.

$$\begin{aligned} &v_o(t)\left[\partial^{1-\alpha}\left(R_p + R_L\right) + \partial^1 C\left(R_s R_p + R_L R_s + R_L R_p\right)\right] \\ &= \partial^{1-\alpha} v_i(t) R_p + \partial^1 v_i(t) C R_s R_p + \delta(t) R_p C R_L v(0) \end{aligned} \tag{16}$$

where ∂^α indicates differentiation of order α.

Now considering the block-pulse function property given in (3) , $v_i(t)$, $v_o(t)$ and $\delta(t)$ can be represented as:

$$v_i(t) = {V_i}^T \phi_M(t) \tag{17}$$
$$v_o(t) = {V_o}^T \phi_M(t) \tag{18}$$
$$\delta(t) = \partial^1 u(t) = U^T \phi_M(t) \tag{19}$$

where $u(t)$ is unit step function, while U^T, ${V_i}^T$ and ${V_i}^T$ are coefficient vectors.

By applying the property given by (6) and using the block pulse signal representations of (17), (18) and (19), equation (16) can be rewritten as:

$$\begin{aligned} &{V_o}^T \phi_M(t)\left[B^{1-\alpha}(R_p+R_L)+B^1 C(R_s R_p+R_L R_s+R_L R_p)\right] \\ &= B^{1-\alpha} {V_i}^T \phi_M(t) R_p + B^1 {V_i}^T \phi_M(t) C R_s R_p \\ &+ B^1 U^T \phi_M(t) R_p C R_L v(0) \end{aligned} \tag{20}$$

Finally, the simple output voltage time domain expression can be written with initial conditions using (18) as below.

$$\begin{aligned} v_o(t) = &\left[B^{1-\alpha} {V_i}^T R_p + B^1 {V_i}^T C R_s R_p + B^1 U^T R_p C R_L v(0)\right] \\ &\left[B^{1-\alpha}(R_p+R_L) + B^1 C(R_s R_p + R_L R_s + R_L R_p)\right]^{-1} \phi_M(t) \end{aligned} \tag{21}$$

The above unique expression (21) is simple and complete for both charging and discharging cycle. When there is a presence of input voltage ($v_i(t) \neq 0$) the equation acts as a charging behaviour and an absence of input voltage ($v_i(t) = 0$), it becomes a discharging equation. This makes it useful during a multi-cycle charging and discharging representation and the transient behaviour of the supercapacitor to a voltage step inputs. Furthermore, the obtained relation will reduce the complexity of identification since the complex fractional-order equation is converted into a simple algebra.

5 Setup for experimentation

The data collection was performed on the circuit shown in Fig. 2 using a DSpace DS2004ADC module. There were three different branded supercapacitors for experimentation, namely AVX, Eaton and Kemet, of capacitance rating of 1.5F. As per objective of the investigation, the different data length for times 10s, 20s, 30s, 40s and 50s cycles were used for each charging or discharging phase (i.e. for a 30s data length it would mean the supercapacitor charging is for 30s and discharging is for 30s). The collection of data for these duration could be justified as most of its applications are based on short bursts of energy storage or discharge. The collected data was sampled at 1000 data points per second. The supply input voltage was 5 volt and $R_L = 270\Omega$.

6 Results and discussion

The non-linear least squares (NLS) technique is adopted to fit the measured data with the estimated output. The NLS can be outlined as below.

$$\min_x \left\| F(x) - y \right\|_2^2 = \min_x \sum_i^n \left(F(x)_i - y_i\right)^2 \tag{22}$$

where x is the vector of unknown parameters (C,α,R_s,R_p), $F(x)$ is the estimated time response and y is the actual response. The subscript i indicates the ith data point at the sampled time t_i.

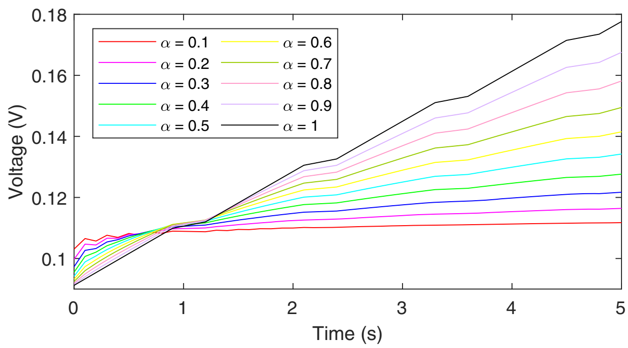

Fig. 3 The effect of changing the α value

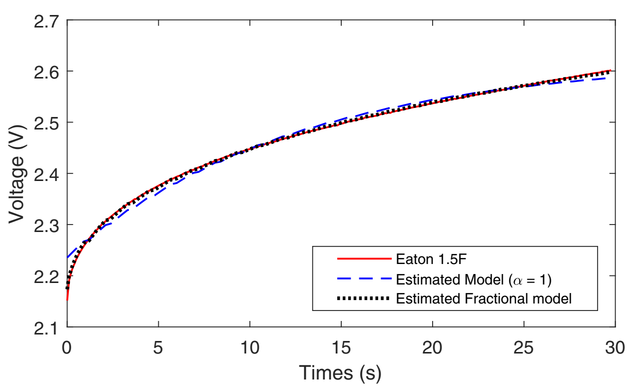

Fig. 4 A comparison of fractional model to a conventional integer model

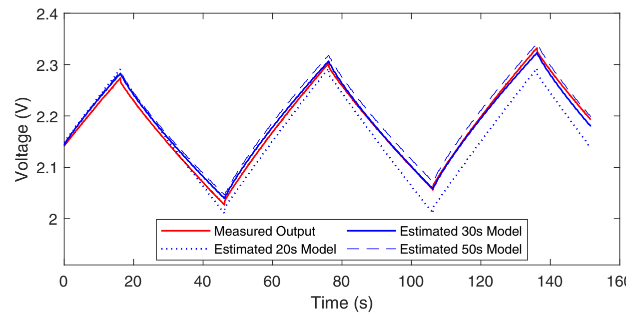

Fig. 5 Estimated model output for Kemet 1.5F supercapacitor of 30s charging/discharging cycle

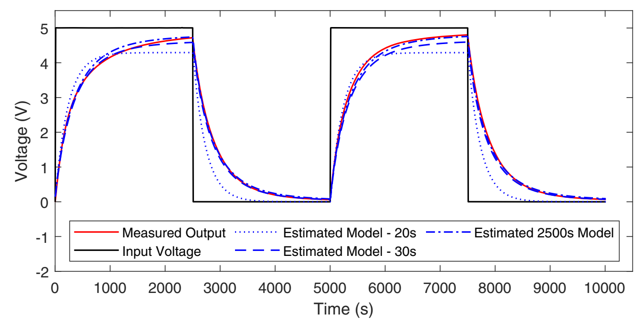

Fig. 6 Comparative results with various time stamp data for Kemet 1.5F

Firstly, the behaviour of the model with the change in the fractional order, α, is studied in Fig. 3. The parameters for C, R_s and R_p were (1.0, 5, 600) respectively which were kept constant, while the α value was varied. It can be seen that with change in the fractional order, the dynamics of the system response to a $5V$ input also changed. Therefore, the importance of using fractional system is outlined. The same can be seen in Fig. 4, the fractional model is able to estimate the behaviour of charging the supercapacitor more accurately than that of a conventional integer based model.

Furthermore, the charging and discharging responses, $v_o(t)$ for input voltage of 0v and 5v were obtained. The input changes from 0v to 5v and vice versa at every 30s. The results obtained from the new expression (21) and NLS fitting, are shown in Fig. 5. The estimated model for parameters (C,α,R_s,R_p) was (0.91, 0.92, 0.04, 2719.66). It shows a close fit to the actual output from Kemet 1.5F supercapacitor. On the same graph, the models from 50s data and 20s data are also plotted for comparisons. The 50s model estimates the 30s time behavior relatively closer than the 20s model, since the 50s falls in region 2 of Fig. 7 where there is very little variance between the parameters.

Further investigation is done to see how the proposed method is able to handle the pronounced curvature. A larger time sampled data is recorded from the same circuit for 2500s charging and 2500s discharging period. The actual outputs (red line) with the input voltages (black line) are plotted in Fig. 6. It is depicted from the Fig. 6, that a longer time frame charging and discharging estimated model of 2500s follows the actual output closely and curvature of response is much more pronounced compared to that for a short time period (Fig.5). This type of change in curvature characteristic is evident due to the rate of change in chemical and physical properties of materials used for making supercapacitor. It is also noted carefully that initial model parameters from the previous Fig. 5's 30s dataset show a close approximation.

Using the proposed technique, the parameter values for time stamps of 10s, 20s, 30s, 40s and 50s were extracted. Then the comparative plots for variation in each parameter were made as illustrated by Fig. 7 to study the variations. Interestingly to note, the parameters varied for each time stamp. We can say that the parameters extracted using a different time cycles are likely not to give a consistent result for new data. However, the variations could be divided in to two regions where region 1 has significant variation while region 2 has a very slight fluctuation in parameters. Parameters of C,α and R_s in region 2 differ utmost by 2% between them but this is not true for the parallel resistance R_p which has a fluctuation of about 20%. It is worth stating that the variance in parallel resistance has a very low impact on the estimated curvature (or very low impact on the estimation error) when its values are significantly large. Based on Fig. 7, it is also

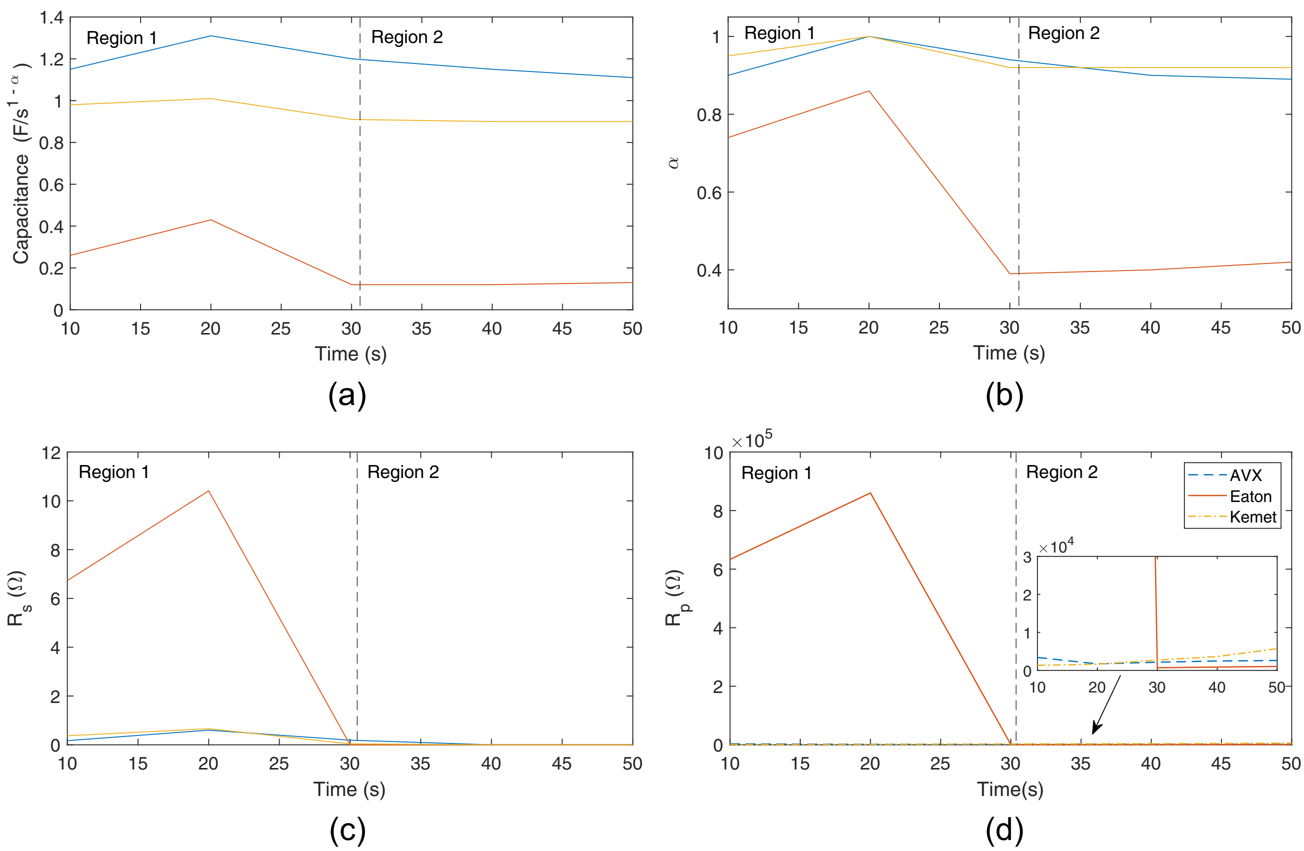

Fig. 7 Individual parameter variation in 10s-50s data

suggested that a time stamp of atleast 30s might be appropriate for estimation purpose of a short span data analysis as it falls in region 2 or the graph where parameters are much more stable.

Looking back at Fig. 6, the parameters collected for 20s (time duration of region 1) shows a significant mismatch of the behavior exhibited by the supercapacitor with longer time frame. However, the parameter from the stable region of Fig. 7 (i.e 30s model parameter) tend to show a much better approximation with longer time frame data. The slight difference in the mismatch of the 30s model to the actual output in Fig. 6 is accounted by the internal phenomenon taking place. This indicates that a model of region 2 is likely to give a close approximation of larger time spanned data as seen in Fig. 6. Furthermore, it would save a lot of time for collecting the large span data and analysing it if an appropriate data length is selected which could demonstrate the behavior for long and short duration both. As noted from above results that atleast a sampled 30s time frame data is sufficient for analysis for short and long duration behavior.

The results from Fig. 7 also suggest that the electrochemical behavior of the supercapacitor may not be consistent for different set of data. The amount of energy it is

Table 1 Extracted Parameters for 1.5F Supercapacitors

Time	Brand	C $(F/s^{1-\alpha})$	α	R_s (Ω)	R_p (Ω)
2500s	Avx	1.13	0.92	4.08	16902.16
	Eaton	1.16	0.97	24.69	22903.33
	Kemet	0.81	0.90	0.00	11036.03

exposed to significantly affects the dynamics and characteristics of output response. To actually see the impact of long term charging and discharging, results are tabulated in Table 1. It is noted that the region 2 parameters of the short time period ranging from 10–50s, are close to the long term charging and discharging for AVX and Kemet branded supercapacitors. However, the Eaton branded supercapacitor demonstrated a vast difference between small and large duration estimated parameters which is likely due to the material properties of the supercapacitor. Further evaluation into the characteristics and parameter variation indicates that a much longer time frame for charging and discharging a supercapacitor estimates parameter which are closer to the rated values.

As explored in [4], the model of individual supercapacitor varies for different manufacturer and capacitance. It is further complimented that models vary with different time stamps and initial charges stored. A significantly high value of R_p could be regarded as an open circuit resulting in only a series R-C circuit. A trend in model simplification (absence of R_p) could be established as values of R_p increases significantly from small time frame data to large time frame data. It could be said that shorter time spans of less than a minute are likely to see an impact of leakage resistance (R_p) present with a less likely impact on the identified curvature in longer time periods (thousands of sec). From Table 1, the three brands parameters obtained for 2500s time span have showed the high R_p value, which becomes insignificant.

7 Conclusions

The proposed technique of block-pulse based identification shows its ability to handle complexity posed by fractal behavior of supercapacitors. Results show that a single transfer function is sufficient to handle a multi-step input and yet show accurate identification. Moreover, investigation on different time stamps of data is also studied, that suggests some indications on variation in parameters and accuracy. Two regions of parameter variation could be seen whereby parameters in region 2 were nearly consistent. Parameters of region 2 may be used to model the behavior at a larger time stamp. Results also suggested that appropriate data length selection is likely to save time in data collection and analysis since a single set of parameters may demonstrate fairly good results for both short and long time span behavior. As from the results, it is suggested that at-least a 30s length of data recording for each phase of charging or discharging is sufficient to conduct behavioral analysis for short and long time span behavior. Such analysis may help in cases where the sample size and recording data is crucial for modeling purpose. The study also suggest that in case for comparison of two capacitors or for comparison of data for the same capacitor, the time stamp used should be constant through out the analysis. Using different duration of data may result in drawing off course conclusions since the behavior of supercapacitor is not same and depends on multiple factors.

References

1. Tsirimokou G, Psychalinos C, Allagui A, Elwakil A (2015) Simple non-impedance-based measuring technique for supercapacitors. Electron Lett 51(21):1699–1701
2. Martynyuk V, Ortigueira M, Fedula M, Savenko O (2018) Fractional model of the electrochemical capacitor relaxation phenomenon. Bull Polish Acad Sci Tech Sci 66(4):68
3. Nayana RLC (2020) Operation and performance of grid connected proton exchange membrane fuel cell with ultra capacitor. Int J Dyn Control 8:189–196
4. Prasad R, Kothari K, Mehta U (2019) Flexible fractional supercapacitor model analyzed in time domain. IEEE Access 7:122626–122633
5. Yang D, Zhu KQ (2010) Start-up flow of a viscoelastic fluid in a pipe with a fractional maxwell's model. Comput Math Appl 60(8):2231–2238
6. Mohebbi A, Abbaszadeh M, Dehghan M (2013) The use of a meshless technique based on collocation and radial basis functions for solving the time fractional nonlinear schrödinger equation arising in quantum mechanics. Eng Anal Boundary Elem 37(2):475–485
7. Fouda M, Elwakil A, Radwan A, Allagui A (2016) Power and energy analysis of fractional-order electrical energy storage devices. Energy 111:785–792
8. Gómez F, Bernal J, Rosales J, Cordova T (2012) Modeling and simulation of equivalent circuits in description of biological systems-a fractional calculus approach. J Electr Bioimpedance 3(1):2–11
9. Garrappa R, Mainardi F, Guido M (2016) Models of dielectric relaxation based on completely monotone functions. Fract Calc Appl Anal 19(5):1105–1160
10. Mescia L, Bia P, Caratelli D (2019) Fractional-calculus-based electromagnetic tool to study pulse propagation in arbitrary dispersive dielectrics. Physica Status Solidi 216(3):1800557
11. Mohammadzadeh A, Kayacan E (2020) A novel fractional-order type-2 fuzzy control method for online frequency regulation in ac microgrid. Eng Appl Artif Intell 90:103483
12. Mohammadzadeh A, Kaynak O (2020) A novel fractional-order fuzzy control method based on immersion and invariance approach. Appl Soft Comput 88:106043
13. Kothari K, Mehta U, Prasad R (2019) Fractional-order system modeling and its applications. J Eng Sci Technol Rev 12(6):1–10
14. Prasad R, Mehta U, Kothari K (2020) Various analytical models for supercapacitors: a mathematical study. Resour Eff Technol 1:1–15
15. Jorcin JB, Orazem ME, Pébère N, Tribollet B (2006) Cpe analysis by local electrochemical impedance spectroscopy. Electrochim Acta 51(8–9):1473–1479
16. Dzielinski, A., Sarwas, G., Sierociuk, D.: Time domain validation of ultracapacitor fractional order model. In: 49th IEEE conference on decision and control (CDC). IEEE (2010). https://doi.org/10.1109/cdc.2010.5717093
17. Freeborn TJ, Elwakil A (2017) Variability of supercapacitor fractional-order parameters extracted from discharging behavior using least squares optimization, pp 1–4 (2017)
18. Freeborn TJ, Allagui A, Elwakil A (2017) Modelling supercapacitors leakage behaviour using a fractional-order model, pp 1–4
19. Freeborn TJ, Maundy B, Elwakil AS (2013) Measurement of supercapacitor fractional-order model parameters from voltage-excited step response. IEEE J Emerg Sel Top Circuits Syst 3(3):367–376. https://doi.org/10.1109/jetcas.2013.2271433
20. Krishnan, G., Das, S., Agarwal, V.: A simple adaptive fractional order model of supercapacitor for pulse power applications. In: 2018 IEEE industry applications society annual meeting (IAS), pp 1–7. IEEE (2018)
21. Quintana JJ, Ramos A, Nuez I (2013) Modeling of an EDLC with fractional transfer functions using mittag-leffler equations. Math Problems Eng 2013:1–7. https://doi.org/10.1155/2013/807034
22. Mitkowski W, Skruch P (2013) Fractional-order models of the supercapacitors in the form of RC ladder networks. Bull Polish Acad Sci Tech Sci 61(3):581–587. https://doi.org/10.2478/bpasts-2013-0059
23. Bertrand N, Sabatier J, Briat O, Vinassa JM (2010) Embedded fractional nonlinear supercapacitor model and its parametric estimation method. IEEE Trans Ind Electron 57(12):3991–4000. https://doi.org/10.1109/tie.2010.2076307
24. Martynyuk V, Ortigueira M (2015) Fractional model of an electrochemical capacitor. Sig Process 107:355–360. https://doi.org/10.1016/j.sigpro.2014.02.021

25. Martynyuk V, Ortigueira M, Fedula M, Savenko O (2018) Methodology of electrochemical capacitor quality control with fractional order model. AEU Int J Electron Commun 91:118–124
26. Buller S, Karden E, Kok D, De Doncker R (2002) Modeling the dynamic behavior of supercapacitors using impedance spectroscopy. IEEE Trans Ind Appl 38(6):1622–1626
27. Quintana JJ, Ramos A, Nuez I (2006) Identification of the fractional impedance of ultracapacitors. IFAC Proc Vol 39(11):432–436. https://doi.org/10.3182/20060719-3-pt-4902.00073
28. Abd-Elhameed W, Youssri Y (2017) Generalized lucas polynomial sequence approach for fractional differential equations. Nonlinear Dyn 89(2):1341–1355
29. Abd-Elhameed W, Youssri Y (2019) Spectral tau algorithm for certain coupled system of fractional differential equations via generalized fibonacci polynomial sequence. Iran J Sci Technol Trans A Sci 43(2):543–554
30. Atta A, Moatimid G, Youssri Y (2019) Generalized fibonacci operational collocation approach for fractional initial value problems. Int J Appl Comput Math 5(1):9
31. Tang Y, Liu H, Wang W, Lian Q, Guan X (2015) Parameter identification of fractional order systems using block pulse functions. Sig Process 107:272–281
32. Prasad V, Kothari K, Mehta U (2020) Parametric identification of nonlinear fractional hammerstein models. Fractal Fract 4(1):1–12
33. Ban S, Zhang J, Zhang L, Tsay K, Song D, Zou X (2013) Charging and discharging electrochemical supercapacitors in the presence of both parallel leakage process and electrochemical decomposition of solvent. Electrochim Acta 90:542–549
34. Zhang Y, Yang H (2011) Modeling and characterization of supercapacitors for wireless sensor network applications. J Power Sources 196(8):4128–4135